Electronic Supplementary Material (ESI) for Inorganic Chemistry Frontiers.
This journal is © the Partner Organisations 2024

Supporting Information

Designing CoS_2-Mo_2C and CoS_2-W_2C hybrids for high-performance supercapacitors and hydrogen evolution reactions

Sajjad Hussain[a,b], Sikandar Aftab[c], Zeesham Abbas[a,b], Iftikhar Hussain[d], Shoyebmohamad F. Shaikh[e], K. Karuppasamy[f,g], Hyun-Seok Kim[h], Jongwan Jung[a,b] , Dhanasekaran Vikraman[h*]

[a] Hybrid Materials Center (HMC), Sejong University, Seoul 05006, Republic of Korea.
[b] Department of Nanotechnology and Advanced Materials Engineering, Sejong University, Seoul 05006, Republic of Korea.
[c] Department of Intelligent Mechatronics Engineering, Sejong University, Seoul 05006, South Korea
[d] Department of Mechanical Engineering, City University of Hong Kong, 83 Tat Chee Avenue, Kowloon, Hong Kong
[e] Department of Chemistry, College of Science, King Saud University, P.O. Box 2455, Riyadh 11451, Saudi Arabia
[f] Department of Chemical and Petroleum Engineering, Khalifa University of Science and Technology, Abu Dhabi, 127788, United Arab Emirates
[g] Emirates Nuclear Technology Center (ENTC), Khalifa University of Science and Technology, Abu Dhabi, 127788, United Arab Emirates
[h] Division of Electronics and Electrical Engineering, Dongguk University-Seoul, Seoul 04620, Republic of Korea.

* Corresponding author's Email: v.j.dhanasekaran@gmail.com

S1. Characterization

Field emission scanning electron microscopy (FESEM) images and energy-dispersive X-ray spectroscopy (EDX) mapping images were obtained using (HITACHI S-4700), 5 kV. The Raman spectroscopy measurements were accomplished using Renishaw Invia RE04, Ar laser - 512 nm at room temperature. The structural properties were characterized by Rigaku X-ray diffractometer with Cu-K_{α} radiation (0.154 nm) at 40 kV and 40 mA in the scanning range of 10-80° (2θ). X-ray powder diffraction (XRD) was conducted with Cu-Kα radiation (0.154 nm) at 40 kV and 40 mA in the scanning range of 5-80° (2θ). The XPS measurements were performed using an Ulvac PHI X-tool spectrometer with Al K_{α} X-ray radiation (1486.6 eV). The atomic structures were characterized by a JEOL-2010F transmission electron microscopy with an accelerating voltage of 200 keV. 3Flex surface characterization analyzer for nitrogen adsorption and desorption measurement at 77 K (Micromeritics, USA).

The HER potential values were converted for reversible hydrogen electrode (RHE) by the given formula: $E(RHE)_{Ag/AgCl} = E\ (vs\ Ag/AgCl) + E^{0}_{(Ag/AgCl)} + 0.0592 \times pH$ for acidic medium and $E(RHE)_{HgO} = E(vs\ Hg/HgO) + E^{0}_{(Hg/HgO)} + 0.0592 \times pH$ for KOH medium.

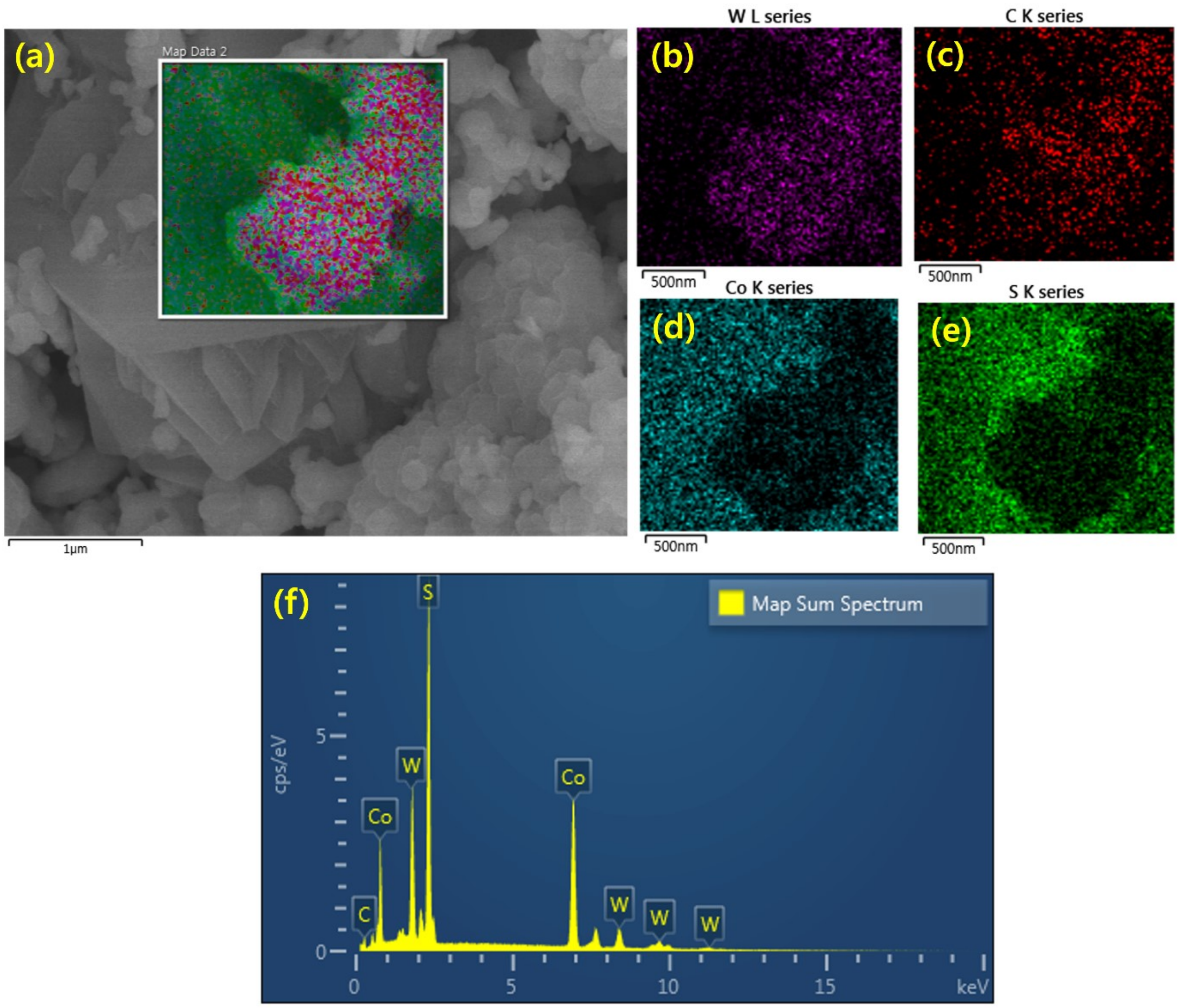

Figure S1. (a) FESEM elemental mapping and (b) W, (c) C, (d) Co and (e) S elements, (f) EDS profile for the CoS_2-W_2C hybrids.

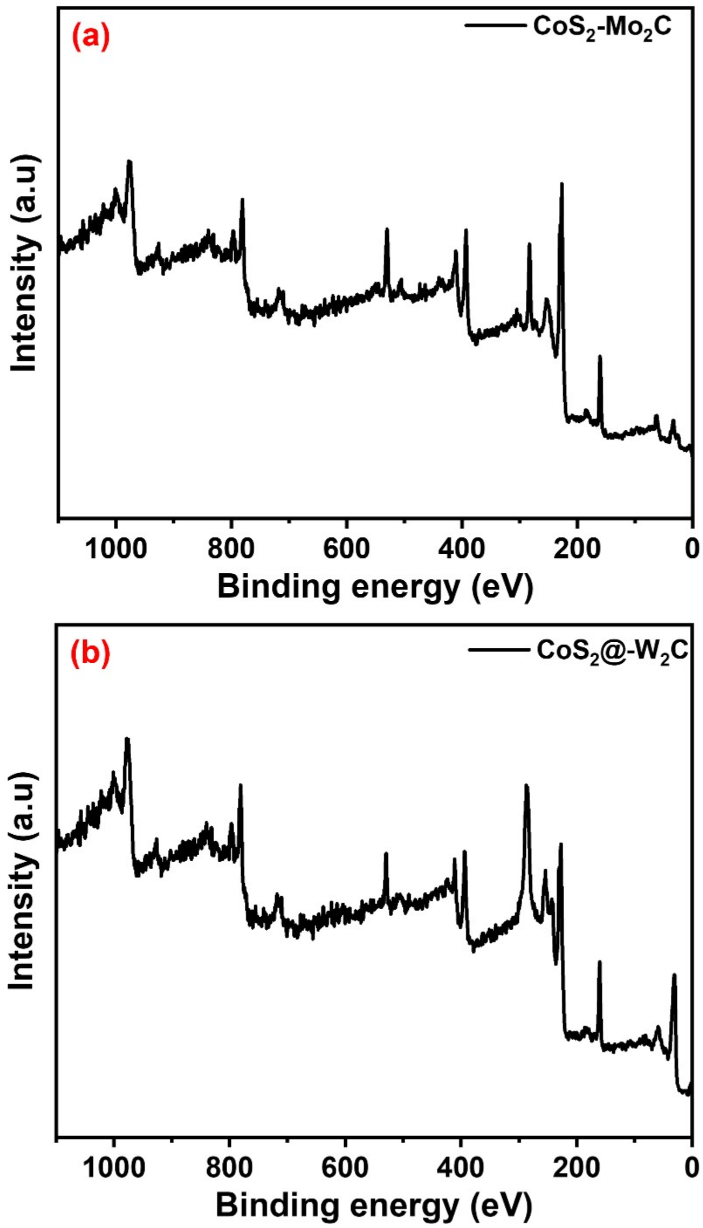

Figure S2. XPS survey spectra for (a) CoS_2-Mo_2C and (b) CoS_2-W_2C hybrids.

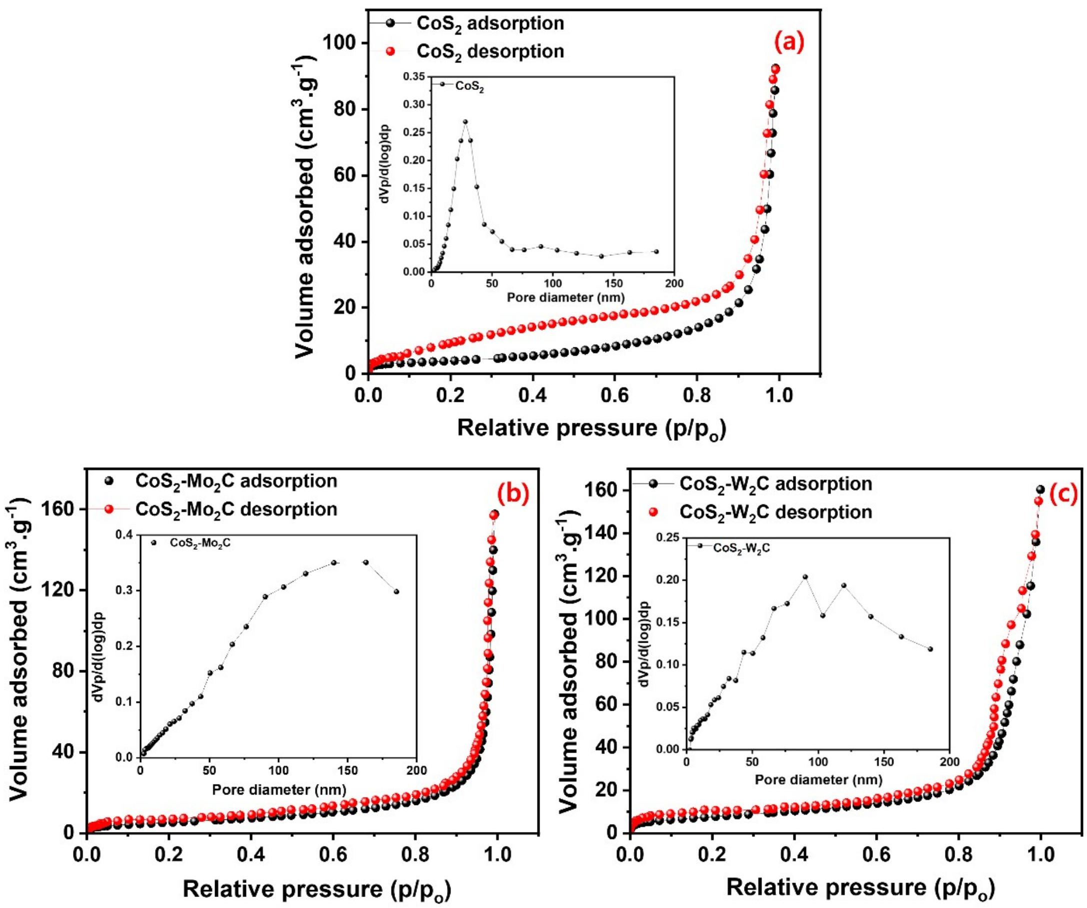

Figure S3. (a-c) BET isotherms curves for (c) CoS_2, (d) CoS_2-Mo_2C and (e) CoS_2-W_2C hybrid nanocomposites (Inset: BJH profiles).

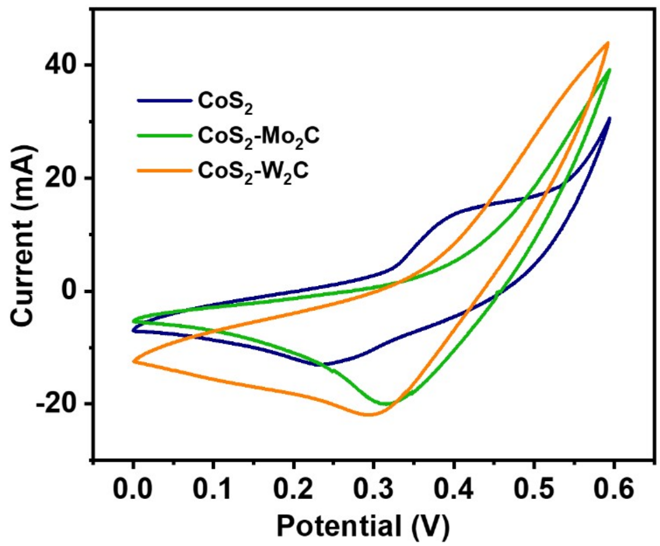

Figure S4. CVs at 100 mV/s for CoS_2, CoS_2-W_2C and CoS_2-Mo_2C electrodes

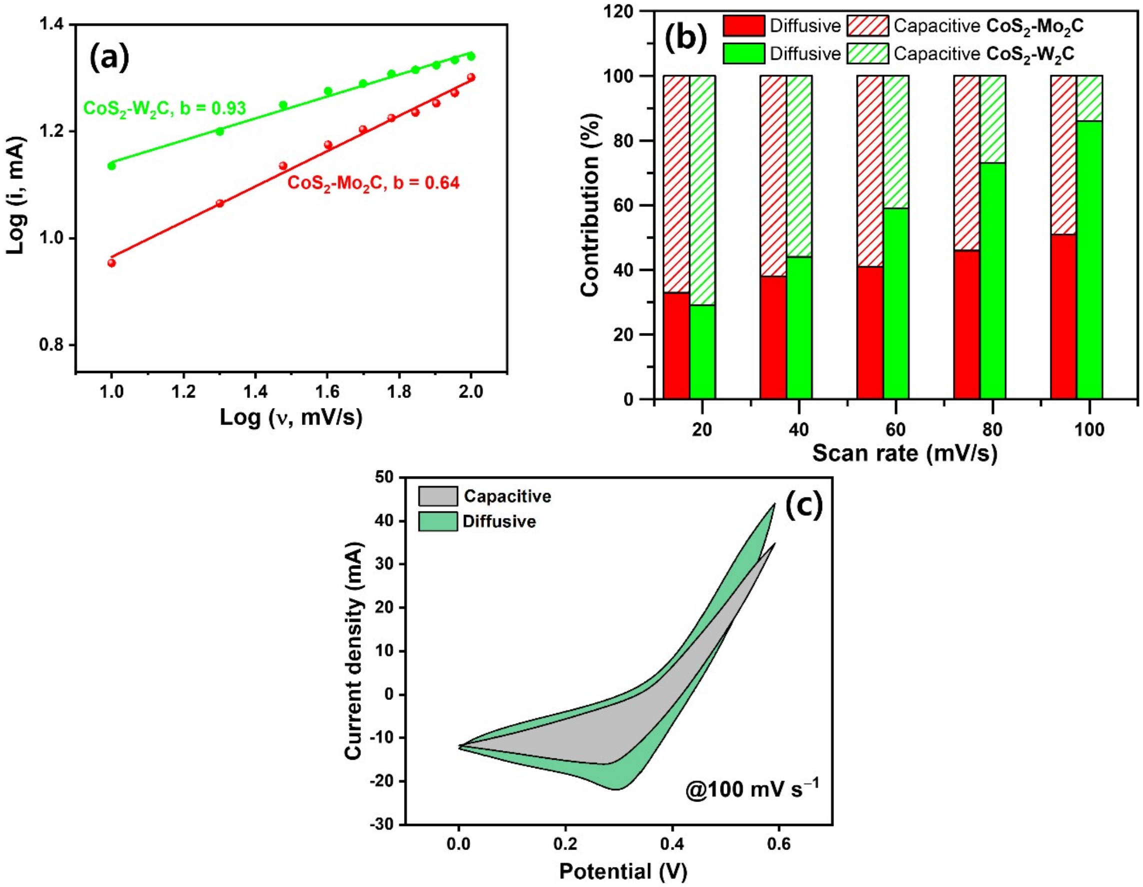

Figure S5. (a) Logarithmic relationship between peak current and scan rates for the hybrid electrodes; (b) Capacitive and diffusive process contribution percentage at different scan rates for hybrid electrodes; (c) Capacitive and diffusion contribution curves for CoS_2-W_2C hybrid electrode at 100 mV/s.

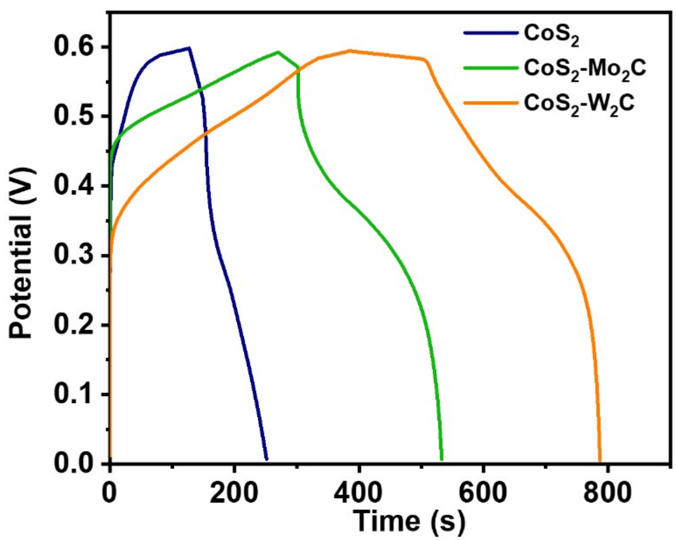

Figure S6. GCDs at 2 A/g for CoS_2, CoS_2-W_2C and CoS_2-Mo_2C electrodes

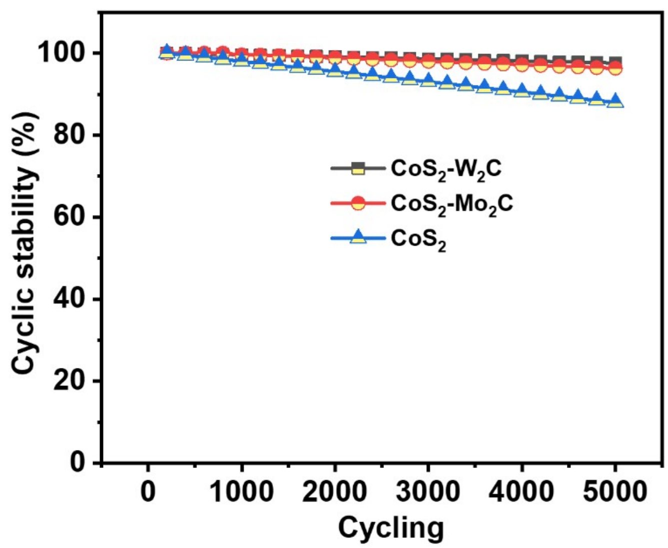

Figure S7. Cycling stability of CoS_2, CoS_2-W_2C and CoS_2-Mo_2C by half-cell

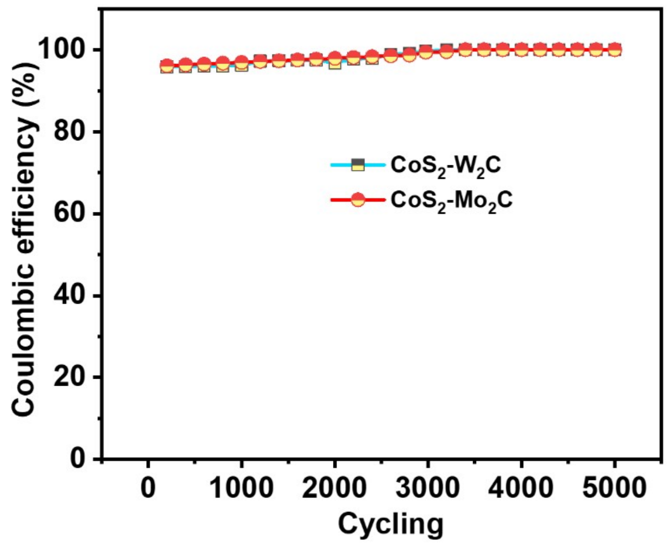

Figure S8. Coulombic efficiency of CoS_2-W_2C and CoS_2-Mo_2C hybrid

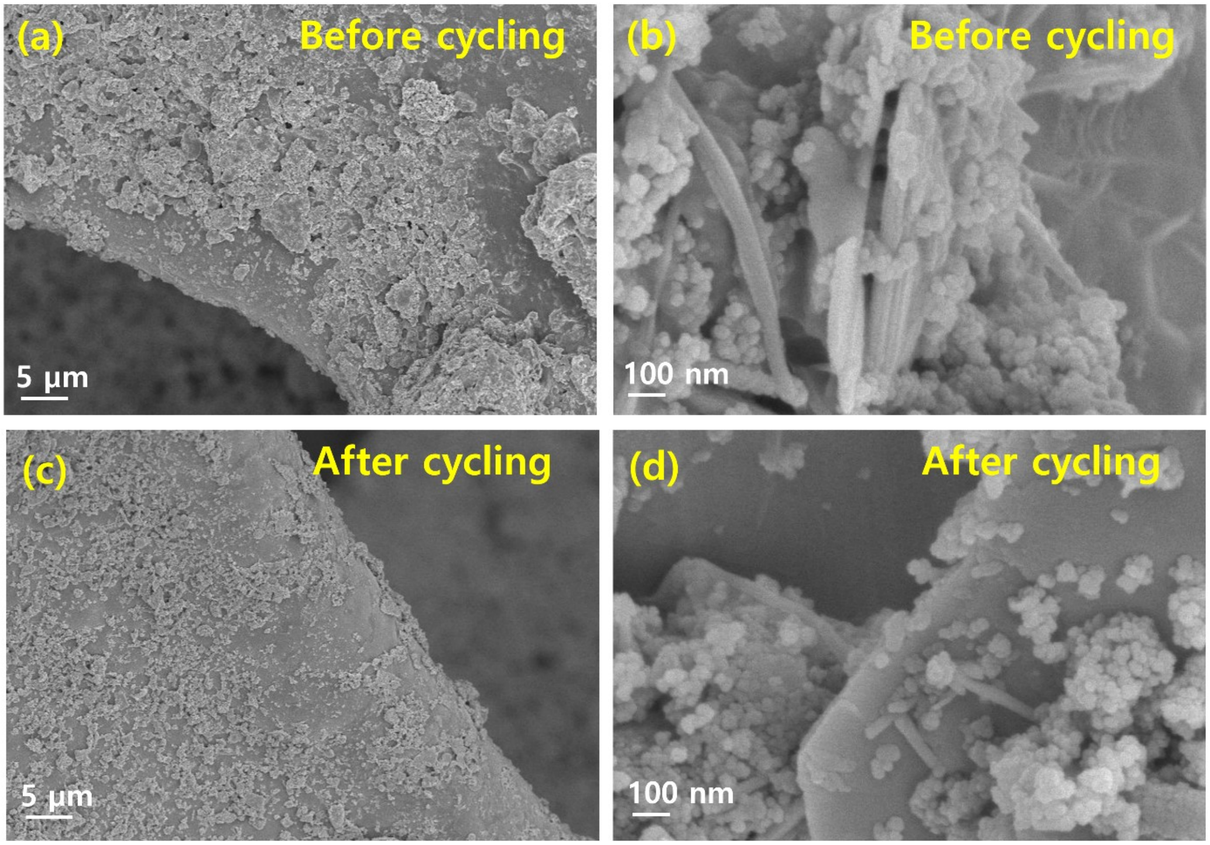

Figure S9. FESEM images (a-b) before and (c-d) after cycling of CoS_2-W_2C coated NF supercapacitor electrode

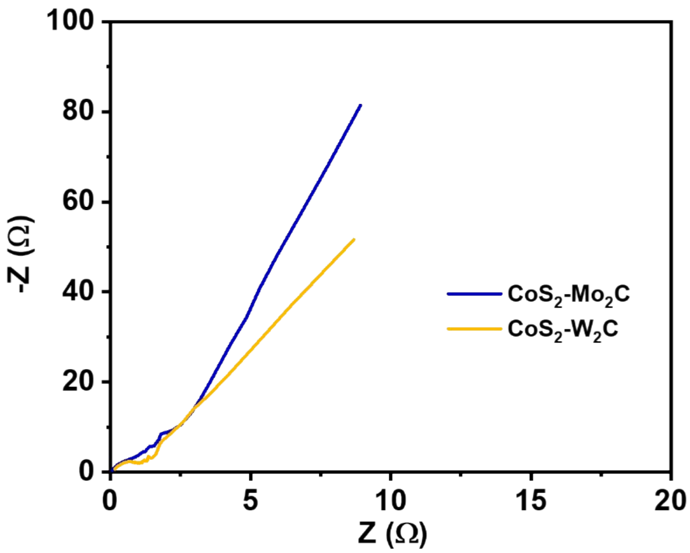

Figure S10. EIS profiles CoS_2-W_2C and CoS_2-Mo_2C ASC devices

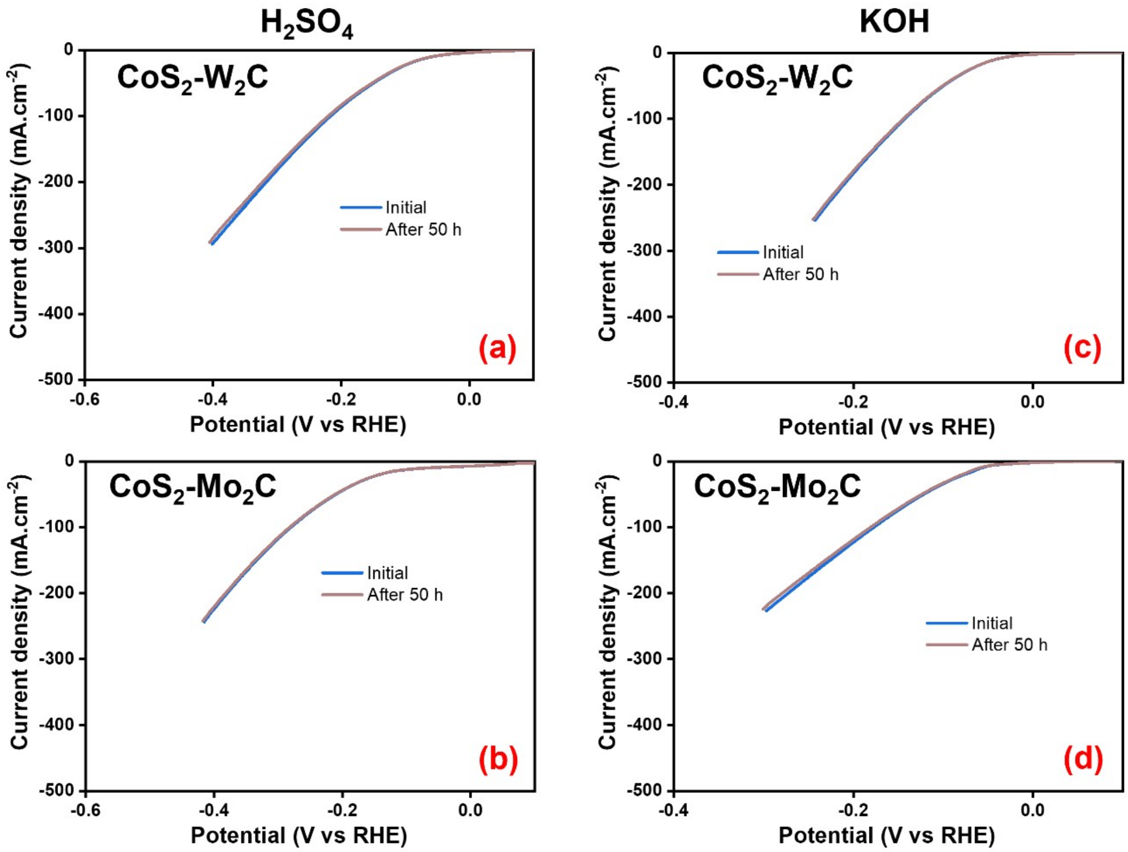

Figure S11. LSV profiles (a,c) CoS_2-W_2C and (b,d) CoS_2-Mo_2C under acid and KOH environment.

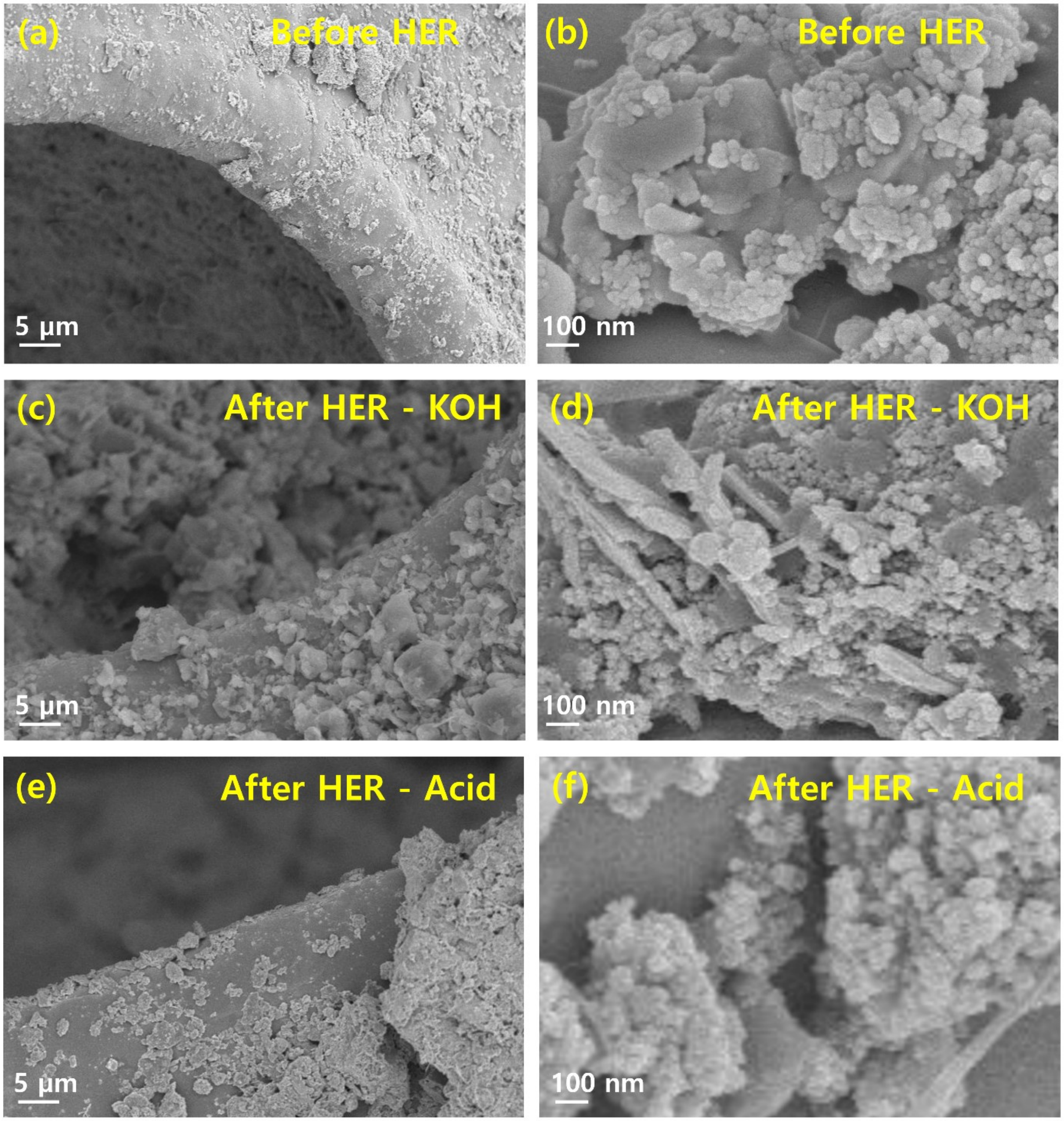

Figure S12. FESEM images (a-b) before HER and after HER in (c-d) KOH and (e-f) acid environment for CoS_2-W_2C electrocatalyst coated NF.

Table S1. Half-cell supercapacitor performances of TMDs and TMCs based electrodes

Electrode materials	Electrolyte	Specific capacitance / capacity	Energy density	Power density	Capacitance retention (%)/cycles	Ref.
CoS_2-W_2C	***3 M KOH***	***720 C/g at 2 A/g***	**-**	**-**	***97/5000***	***This work***
3Dgraphene/ MoS_2 composite	1.0 M Na_2SO_4	410 $F \cdot g^{-1}$ @ 1 $A \cdot g^{-1}$	-	-	80.3/10000	1
Mo_2C/MoS_2 hybrid	1 M KOH	1040 $F \cdot g^{-1}$ @ 0.5 $A \cdot g^{-1}$	-	-	94/5000	2
W_2C/MoS_2 hybrid	1 M KOH	681 $F \cdot g^{-1}$ @ 0.5 $A \cdot g^{-1}$	-	-	90/5000	2
WS_2/RGO hybrids	1.0 M Na_2SO_4	350 F/g@ 2mV/s	~49 Wh/kg	-	-	3
WS_2@MXene/GO	1 KOH	1111 $F \cdot g^{-1}$ @ 2 $A \cdot g^{-1}$	-	-	97.15/5000	4
3D graphene-MoS_2 hybrid	1.0 M KOH	169.3 F/g	28.43 Wh/Kg	10.18 W/kg	-	5
$MoSe_2$-Mo_2C hybrid nanoarrays	1 M KOH	850 $F \cdot g^{-1}$ @ 2.5 $A \cdot g^{-1}$	-	-	98/10000	6
Mo_2C/NCF	6.0 M KOH	1250 $F \cdot g^{-1}$ @ 1 $A \cdot g^{-1}$	-	-	100/500	7
MXene-$NiCo_2S_4$@ NF	3 M KOH	1147.47 $F \cdot g^{-1}$ @ 1 $A \cdot g^{-1}$	-	-	80.4/3000	8
MoS_2/CNS	1 M Na_2SO_4	108 F g^{-1} @ 1 A g^{-1}	74 Wh/kg	3700 W/Kg	-	9
MoS_2/MXene nanohybrid	3 M KOH	583 $F \cdot g^{-1}$ @ 1 $A \cdot g^{-1}$	-	-	82.5/3000	10
MoS_2/MWCNT	1 M Na_2SO_4	452.7 F g^{-1} @ 1 A g^{-1}	-	-	95.8/ 1000	11
$NiCo_2S_4$-g-MoS_2	1.0 M KOH	1270 F g^{-1} @1 A g^{-1}	-	-	94.8/4000	12
MoS_2-graphene	1.0 M KOH	756 $F \cdot g^{-1}$ @ 0.5 $A \cdot g^{-1}$	6 Wh/Kg	125 W/kg	88/10000	13

Table S2. Asymmetric supercapacitors performances of TMDs and TMCs based electrodes

Electrode materials	**Specific capacitance**	**Energy density**	**Power density**	**Capacitance retention (%)/cycles**	**Ref.**
CoS_2-W_2C	***423 F/g at 2 A/g***	***150 Wh/Kg***	***4.5 kW/Kg***	***94.1/5000***	***This work***
MXene/$MoSe_2$	350 $F\cdot g^{-1}$ @ 1 $A\cdot g^{-1}$	48 Wh/Kg	500 W/kg	93/5000	14
MXene-$NiCo_2S_4$@NF	-	27.24 Wh/Kg	0.48 kW/kg	-	8
MXene/CuS	49.3 $F\cdot g^{-1}$ @ 0.5 $A\cdot g^{-1}$	15.4 Wh/Kg	750.2 W/kg	82.4/5000	15
1T-MoS_2/ MXene	386.7$F\cdot g^{-1}$ @ 1 $A\cdot g^{-1}$	-	-	91.1/20000	16
MXene/$NiCo_2S_4$	621$F\cdot g^{-1}$ @ 1 $A\cdot g^{-1}$	72.82 Wh/Kg	0.635k W/Kg	90.88/20000	17
1T-VS_2/MXene Hybrid	115.7 $F\cdot g^{-1}$ @ 0.8 $A\cdot g^{-1}$	41.13 Wh/Kg	793.50 W/kg	85/5000	18
$Cu_{0.5}Co_{0.5}Se_2$// MXene	321 $F\cdot g^{-1}$ @ 1 $A\cdot g^{-1}$	84.19 Wh/Kg	715.12 W/kg	91.1/10000	19
MXene-MoO_2	3 F cm^{-3} @ 2 mV s^{-1}	9.7 mW h cm-3	0.198 W cm^{-3}	88/10000	20
$NiMoO_4$/$Ti_3C_2T_x$	137.3 $F\cdot g^{-1}$ @ 0.5 $A\cdot g^{-1}$	33.36 Wh/Kg	400.08 W/kg	72.6/10000	21
Ti_3C_2/Ni-Co-Al-LDH	128.89 $F\cdot g^{-1}$ @ 0.5 $A\cdot g^{-1}$	23.6 Wh/Kg	6.93 kW/kg	97.8/10000	22
NiCoS/d-Ti_3C_2	95.2 $F\cdot g^{-1}$ @ 0.5 $A\cdot g^{-1}$	22.6 Wh/Kg	0.4 kW/kg	91.2/10000	23
graphene/MXene hydrogel	226.7 $F\cdot g^{-1}$ @ 1 $A\cdot g^{-1}$	9.3 Wh/Kg	500 W/kg	-	24
$NiCo_2$-LDHs@MXene/rGO	240 $F\cdot g^{-1}$ @ 0.5 $A\cdot g^{-1}$	65.3 Wh/Kg	700 W/kg	92.8/10000	25
MXene/$MoSe_2$ /ASC	156.3 $F\cdot g^{-1}$ @ 0.5 $A\cdot g^{-1}$	55.6 Wh/Kg	800.3 W/kg	94.1/5000	26
V_2NT_x MXene	112.8 $F.g^{-1}$ @1.85 mA/cm^2	15.66 Wh/Kg	3748.4 W/kg	96/10000	27
MXene@Ni-Mn LDH	56 $F\cdot g^{-1}$ @ 1 $A\cdot g^{-1}$	44.7 Wh/Kg	800 W/kg	90.3/5000	28
Ni–S/d-Ti_3C_2 nanohybrid	69.4 $c\cdot g^{-1}$ @ 0.5 $A\cdot g^{-1}$	5.1 Wh/Kg	10k W/kg	71.4/10000	29

$Ni_{1.5}Co_{1.5}S_{4-5}$@Ti_3C_2	140 $A \cdot g^{-1}$ @ 1 $A \cdot g^{-1}$	49.8 Wh/Kg	800 W/kg	90/8000	[30]

Table S3. HER catalytic performances TMDs and TMCs-based electrocatalysts

Electrocatalyst	Electrolyte	η (mV)	Tafel Slope ($mV\cdot dec^{-1}$)	j_0 ($mA\cdot cm^{-2}$)	Ref
CoS_2-W_2C	**1 M KOH**	**42**	**27**	**1.35**	**This work**
CoS_2-W_2C	**0.5 M H_2SO_4**	**50**	**42**	**1.2**	
Reduced GO-Mo_2C composites	0.5 M H_2SO_4	206 @ 10 mA/cm^2	52	-	31
$MoSe_2$/$NiSe_2$ composite nanowires	0.5 M H_2SO_4	249 @ 100 mA/cm^2	46.9	-	32
MoO_2/α-Mo_2C heterojunction	0.5 M H_2SO_4 & 1 M KOH	152 & -100@ 10 mA/cm^2	65 & 50	4.42×10^{-2}	33
Mo_2C Nanoparticles	0.5 M H_2SO_4 & 1 M KOH	180 & 210@ 10 mA/cm^2	49 & 48	3×10^{-3}	34
WS_2/W_2C heterostructure	0.5 M H_2SO_4	126@ 10 mA/cm^2	68	0.501	35
$MoSe_2$@MoS_2	0.5 M H_2SO_4	161 @ 10 mA/cm^2	60	-	36
Mo_2C/mesoporous carbon	0.1 M KOH	165 @ 10 mA/cm^2	63.3	-	37
Mo_2C/ N doped carbon nanotubes	0.5 M H_2SO_4	147@ 10 mA/cm^2	71	72.7@200 mV	38
MoC-Mo_2C Heteronanowires	0.5 M H_2SO_4 & 1 M KOH	126 & 120@ 10 mA/cm^2	43 & 42	1.1×10^{-2}	39
$CoSe_2$/$MoSe_2$ heterostructures	1 M KOH	218 @ 10 mA/cm^2	76	-	40
Mo_2C/CNT	1.0 M $HClO_4$	64@ 1 mA/cm^2	52.2	1.4×10^{-2}	41
$MoSe_2$/Bi_2Se_3 hybrids	0.5 M H_2SO_4	300 mV @ 85 mA/cm^2	44	-	42
MoP/Mo_2C@C	0.5 M H_2SO_4	89@ 10 mA/cm^2	45	0.215	43
Mo_2C/MoS_2	0.5 M H_2SO_4 & 1 M KOH	93 & 98 @ 10 mA/cm^2	67 & 68	0.952 & 1.32	2
MoSSe Nanoflake	0.5 M H_2SO_4	164 @ 10 mA/cm^2	48	-	44
MoSSe@rGO composite	0.5 M H_2SO_4	135 @ 5mA/cm^2	51	-	45
Mo_2C Nanoparticles/ N doped porous carbon nanofibers	0.5 M H_2SO_4 & 1 M KOH	85 & 90@ 1 mA/cm^2	68 & 60.2	0.178	46
Mo_2C/Graphene Nanoribbons	0.5 M H_2SO_4 & 1 M KOH	167 & 217@ 10 mA/cm^2	63 & 64	-	47

Mo_2C/CNT-graphene	0.5 M H_2SO_4	130@ 10 mA/cm^2	58	6.20×10^{-2}	48
MoCx nano- octahedrons	0.5 M H_2SO_4 and 1M KOH	142 & 151@ 10 mA/cm^2	53 & 59	0.023 & 0.029	49

References

1. T. Sun, Z. Li, X. Liu, L. Ma, J. Wang and S. Yang, Facile construction of 3D graphene/MoS_2 composites as advanced electrode materials for supercapacitors, *J. Power Sources*, 2016, **331**, 180-188.
2. S. Hussain, I. Rabani, D. Vikraman, A. Feroze, M. Ali, Y.-S. Seo, W. Song, K.-S. An, H.-S. Kim and S.-H. Chun, MoS2@ X2C (X= Mo or W) hybrids for enhanced supercapacitor and hydrogen evolution performances, *Chemical Engineering Journal*, 2021, **421**, 127843.
3. S. Ratha and C. S. Rout, Supercapacitor electrodes based on layered tungsten disulfide-reduced graphene oxide hybrids synthesized by a facile hydrothermal method, *ACS applied materials & interfaces*, 2013, **5**, 11427-11433.
4. S. Hussain, D. Vikraman, Z. A. Sheikh, M. T. Mehran, F. Shahzad, K. M. Batoo, H.-S. Kim, D.-K. Kim, M. Ali and J. Jung, WS2-embedded MXene/GO hybrid nanosheets as electrodes for asymmetric supercapacitors and hydrogen evolution reactions, *Chemical Engineering Journal*, 2023, **452**, 139523.
5. K. Singh, S. Kumar, K. Agarwal, K. Soni, V. R. Gedela and K. Ghosh, Three-dimensional Graphene with MoS 2 Nanohybrid as Potential Energy Storage/Transfer Device, *Scientific reports*, 2017, **7**, 9458.
6. D. Vikraman, S. Hussain, K. Karuppasamy, A. Feroze, A. Kathalingam, A. Sanmugam, S.-H. Chun, J. Jung and H.-S. Kim, Engineering the novel MoSe2-Mo2C hybrid nanoarray electrodes for energy storage and water splitting applications, *Applied Catalysis B: Environmental*, 2020, **264**, 118531.
7. K. J. Samdani, D. W. Joh and K. T. Lee, Molybdenum carbide nanoparticle-decorated 3D nitrogen-doped carbon flowers as an efficient electrode for high-performance, all-solid-state symmetric supercapacitors, *J. Alloys Compd.*, 2018, **748**, 134-144.

8. H. Li, X. Chen, E. Zalnezhad, K. Hui, K. Hui and M. J. Ko, 3D hierarchical transition-metal sulfides deposited on MXene as binder-free electrode for high-performance supercapacitors, *Journal of Industrial and Engineering Chemistry*, 2020, **82**, 309-316.
9. T. N. Khawula, K. Raju, P. J. Franklyn, I. Sigalas and K. I. Ozoemena, Symmetric pseudocapacitors based on molybdenum disulfide (MoS 2)-modified carbon nanospheres: correlating physicochemistry and synergistic interaction on energy storage, *Journal of Materials Chemistry A*, 2016, **4**, 6411-6425.
10. B. Kirubasankar, M. Narayanasamy, J. Yang, M. Han, W. Zhu, Y. Su, S. Angaiah and C. Yan, Construction of heterogeneous 2D layered MoS2/MXene nanohybrid anode material via interstratification process and its synergetic effect for asymmetric supercapacitors, *Applied Surface Science*, 2020, **534**, 147644.
11. K.-J. Huang, L. Wang, J.-Z. Zhang, L.-L. Wang and Y.-P. Mo, One-step preparation of layered molybdenum disulfide/multi-walled carbon nanotube composites for enhanced performance supercapacitor, *Energy*, 2014, **67**, 234-240.
12. J. Shen, P. Dong, R. Baines, X. Xu, Z. Zhang, P. M. Ajayan and M. Ye, Controlled synthesis and comparison of NiCo 2 S 4/graphene/2D TMD ternary nanocomposites for high-performance supercapacitors, *Chemical Communications*, 2016, **52**, 9251-9254.
13. D. Vikraman, K. Karuppasamy, S. Hussain, A. Kathalingam, A. Sanmugam, J. Jung and H. S. Kim, One-pot facile methodology to synthesize MoS_2-graphene hybrid nanocomposites for supercapacitors with improved electrochemical capacitance, *Compos. Part B-Eng.*, 2019, **161**, 555-563.
14. S. Hussain, I. Rabani, D. Vikraman, T. Mehran, F. Shahzad, Y. S. Seo, H. S. Kim and J. Jung, Designing the MXene/molybdenum diselenide hybrid nanostructures for high-performance symmetric supercapacitor and hydrogen evolution applications, *International Journal of Energy Research*, 2021, **45**, 18770-18785.
15. Z. Pan, F. Cao, X. Hu and X. Ji, A facile method for synthesizing CuS decorated Ti3C2 MXene with enhanced performance for asymmetric supercapacitors, *Journal of Materials Chemistry A*, 2019, **7**, 8984-8992.

16. X. Wang, H. Li, H. Li, S. Lin, W. Ding, X. Zhu, Z. Sheng, H. Wang, X. Zhu and Y. Sun, 2D/2D 1T-MoS2/Ti3C2 MXene Heterostructure with Excellent Supercapacitor Performance, *Advanced Functional Materials*, 2020, **30**, 0190302.
17. Y. Li, K. Donatien-Pascal and X. Jin, In situ growth of Chrysanthemum-like NiCo2S4 on MXene for High-performance Supercapacitors and Non-enzymatic H2O2 Sensor, *Dalton Transactions*, 2020.
18. A. Sharma, P. Mane, B. Chakraborty and C. S. Rout, 1T-VS2/MXene Hybrid as a Superior Electrode Material for Asymmetric Supercapacitors: Experimental and Theoretical Investigations, *ACS Applied Energy Materials*, 2021, **4**, 14198-14209.
19. Y. A. Dakka, J. Balamurugan, R. Balaji, N. H. Kim and J. H. Lee, Advanced Cu0. 5Co0. 5Se2 nanosheets and MXene electrodes for high-performance asymmetric supercapacitors, *Chemical Engineering Journal*, 2020, **385**, 123455.
20. L. Zhang, G. Yang, Z. Chen, D. Liu, J. Wang, Y. Qian, C. Chen, Y. Liu, L. Wang and J. Razal, MXene coupled with molybdenum dioxide nanoparticles as 2D-0D pseudocapacitive electrode for high performance flexible asymmetric micro-supercapacitors, *Journal of Materiomics*, 2020, **6**, 138-144.
21. Y. Wang, J. Sun, X. Qian, Y. Zhang, L. Yu, R. Niu, H. Zhao and J. Zhu, 2D/2D heterostructures of nickel molybdate and MXene with strong coupled synergistic effect towards enhanced supercapacitor performance, *Journal of Power Sources*, 2019, **414**, 540-546.
22. R. Zhao, M. Wang, D. Zhao, H. Li, C. Wang and L. Yin, Molecular-level heterostructures assembled from titanium carbide MXene and Ni–Co–Al layered double-hydroxide nanosheets for all-solid-state flexible asymmetric high-energy supercapacitors, *ACS Energy Letters*, 2017, **3**, 132-140.
23. Y. Luo, Y. Tian, Y. Tang, X. Yin and W. Que, 2D hierarchical nickel cobalt sulfides coupled with ultrathin titanium carbide (MXene) nanosheets for hybrid supercapacitors, *Journal of Power Sources*, **482**, 228961.
24. L. Zhang and S. W. Or, Self-assembled three-dimensional macroscopic graphene/MXene-based hydrogel as electrode for supercapacitor, *APL Materials*, 2020, **8**, 091101.

25. J. Zheng, X. Pan, X. Huang, D. Xiong, Y. Shang, X. Li, N. Wang, W.-M. Lau and H. Y. Yang, Integrated MXene-based Aerogel Composite: Componential and Structural Engineering towards Enhanced Performance Stability of Hybrid Supercapacitor, *Chemical Engineering Journal*, 2020, 125197.
26. X. Chen, J. Zhu, J. Cai, Y. Zhang and X. Wang, Nanosheets assembled layered MXene/MoSe2 nanohybrid positive electrode materials for high-performance asymmetric supercapacitors, *Journal of Energy Storage*, 2021, **40**, 102721.
27. S. Venkateshalu, J. Cherusseri, M. Karnan, K. S. Kumar, P. Kollu, M. Sathish, J. Thomas, S. K. Jeong and A. N. Grace, New Method for the Synthesis of 2D Vanadium Nitride (MXene) and Its Application as a Supercapacitor Electrode, *ACS omega*, 2020, **5**, 17983-17992.
28. W. Wang, D. Jiang, X. Chen, K. Xie, Y. Jiang and Y. Wang, A sandwich-like nano-micro LDH-MXene-LDH for high-performance supercapacitors, *Applied Surface Science*, 2020, 145982.
29. Y. Luo, C. Yang, Y. Tian, Y. Tang, X. Yin and W. Que, A long cycle life asymmetric supercapacitor based on advanced nickel-sulfide/titanium carbide (MXene) nanohybrid and MXene electrodes, *Journal of Power Sources*, 2020, **450**, 227694.
30. X. He, T. Bi, X. Zheng, W. Zhu and J. Jiang, Nickel cobalt sulfide nanoparticles grown on titanium carbide MXenes for high-performance supercapacitor, *Electrochimica Acta*, 2020, **332**, 135514.
31. K. Ojha, S. Saha, H. Kolev, B. Kumar and A. K. Ganguli, Composites of graphene-Mo2C rods: highly active and stable electrocatalyst for hydrogen evolution reaction, *Electrochimica Acta*, 2016, **193**, 268-274.
32. L. Zhang, T. Wang, L. Sun, Y. Sun, T. Hu, K. Xu and F. Ma, Hydrothermal synthesis of 3D hierarchical $MoSe_2/NiSe_2$ composite nanowires on carbon fiber paper and their enhanced electrocatalytic activity for the hydrogen evolution reaction, *J. Mater. Chem. A*, 2017, **5**, 19752-19759.
33. Y. Liu, B. Huang and Z. Xie, Hydrothermal synthesis of core-shell MoO2/α-Mo2C heterojunction as high performance electrocatalyst for hydrogen evolution reaction, *Applied Surface Science*, 2018, **427**, 693-701.

34. D. Wang, J. Wang, X. Luo, Z. Wu and L. Ye, In situ preparation of Mo2C nanoparticles embedded in ketjenblack carbon as highly efficient electrocatalysts for hydrogen evolution, *ACS Sustainable Chemistry & Engineering*, 2017, **6**, 983-990.
35. Y. Li, X. Wu, H. Zhang and J. Zhang, Interface Designing over WS2/W2C for Enhanced Hydrogen Evolution Catalysis, *ACS Applied Energy Materials*, 2018, **1**, 3377-3384.
36. X. Ren, Q. Wei, P. Ren, Y. Wang and R. Chen, Synthesis of flower-like $MoSe_2$@MoS_2 nanocomposites as the high efficient water splitting electrocatalyst, *Mater. Lett.*, 2018, **231**, 213-216.
37. M. Qamar, A. Adam, B. Merzougui, A. Helal, O. Abdulhamid and M. Siddiqui, Metal–organic framework-guided growth of Mo 2 C embedded in mesoporous carbon as a high-performance and stable electrocatalyst for the hydrogen evolution reaction, *Journal of Materials Chemistry A*, 2016, **4**, 16225-16232.
38. K. Zhang, Y. Zhao, D. Fu and Y. Chen, Molybdenum carbide nanocrystal embedded N-doped carbon nanotubes as electrocatalysts for hydrogen generation, *Journal of Materials Chemistry A*, 2015, **3**, 5783-5788.
39. H. Lin, Z. Shi, S. He, X. Yu, S. Wang, Q. Gao and Y. Tang, Heteronanowires of MoC–Mo 2 C as efficient electrocatalysts for hydrogen evolution reaction, *Chemical science*, 2016, **7**, 3399-3405.
40. G. Zhao, P. Li, K. Rui, Y. Chen, S. X. Dou and W. Sun, $CoSe_2$/$MoSe_2$ Heterostructures with Enriched Water Adsorption/Dissociation Sites towards Enhanced Alkaline Hydrogen Evolution Reaction, *Chem. Eur. J.*, 2018, **24**, 11158-11165.
41. W.-F. Chen, C.-H. Wang, K. Sasaki, N. Marinkovic, W. Xu, J. Muckerman, Y. Zhu and R. Adzic, Highly active and durable nanostructured molybdenum carbide electrocatalysts for hydrogen production, *Energy & Environmental Science*, 2013, **6**, 943-951.
42. J. Yang, C. Wang, H. Ju, Y. Sun, S. Xing, J. Zhu and Q. Yang, Integrated Quasiplane Heteronanostructures of $MoSe_2$/Bi_2Se_3 Hexagonal Nanosheets: Synergetic Electrocatalytic Water Splitting and Enhanced Supercapacitor Performance, *Adv. Funct. Mater.*, 2017, **27**, 1703864.
43. L.-N. Zhang, S.-H. Li, H.-Q. Tan, S. U. Khan, Y.-Y. Ma, H.-Y. Zang, Y.-H. Wang and Y.-G. Li, MoP/Mo2C@ C: a new combination of electrocatalysts for highly efficient hydrogen

evolution over the entire pH range, *ACS applied materials & interfaces*, 2017, **9**, 16270-16279.

44. Q. Gong, L. Cheng, C. Liu, M. Zhang, Q. Feng, H. Ye, M. Zeng, L. Xie, Z. Liu and Y. Li, Ultrathin MoS2 (1–x) Se2 x alloy nanoflakes for electrocatalytic hydrogen evolution reaction, *Acs Catalysis*, 2015, **5**, 2213-2219.
45. B. Konkena, J. Masa, W. Xia, M. Muhler and W. Schuhmann, MoSSe@ reduced graphene oxide nanocomposite heterostructures as efficient and stable electrocatalysts for the hydrogen evolution reaction, *Nano Energy*, 2016, **29**, 46-53.
46. H. Wang, C. Sun, Y. Cao, J. Zhu, Y. Chen, J. Guo, J. Zhao, Y. Sun and G. Zou, Molybdenum carbide nanoparticles embedded in nitrogen-doped porous carbon nanofibers as a dual catalyst for hydrogen evolution and oxygen reduction reactions, *Carbon*, 2017, **114**, 628-634.
47. W. Gao, Y. Shi, Y. Zhang, L. Zuo, H. Lu, Y. Huang, W. Fan and T. Liu, Molybdenum carbide anchored on graphene nanoribbons as highly efficient all-pH hydrogen evolution reaction electrocatalyst, *ACS Sustainable Chemistry & Engineering*, 2016, **4**, 6313-6321.
48. D. H. Youn, S. Han, J. Y. Kim, J. Y. Kim, H. Park, S. H. Choi and J. S. Lee, Highly active and stable hydrogen evolution electrocatalysts based on molybdenum compounds on carbon nanotube–graphene hybrid support, *ACS nano*, 2014, **8**, 5164-5173.
49. H. B. Wu, B. Y. Xia, L. Yu, X.-Y. Yu and X. W. D. Lou, Porous molybdenum carbide nano-octahedrons synthesized via confined carburization in metal-organic frameworks for efficient hydrogen production, *Nature communications*, 2015, **6**, 6512.